IEEE Access
Multidisciplinary | Rapid Review | Open Access Journal

Received May 19, 2020, accepted June 15, 2020, date of publication June 24, 2020, date of current version July 3, 2020.

Digital Object Identifier 10.1109/ACCESS.2020.3004557

The Prosumer Energy Management Method Based on Smart Load

GANG MA, JIE LYU, YING WANG, JIAN ZHANG, AND JIE XU
School of Electrical and Automation Engineering, Nanjing Normal University, Nanjing 210097, China

Corresponding author: Gang Ma (nnumg@njnu.edu.cn)

This work was supported in part by the National Natural Science Foundation of China under Grant 51607093.

ABSTRACT With the development of household photovoltaic and electric vehicles, household electricity units are no longer traditional power consumers, but also power producers, which are defined as Prosumers. In order to solve the problems of Prosumer energy circulation and its grid-connected control, this paper proposes a new Prosumer energy management method. First, PSO algorithm is used for day-ahead optimization to smooth the load curve of prosumer. Then based on the Smart Load (SL) which can control the active power flexibly, the real-time energy management method of Prosumer is proposed. At last, the multi-Prosumers grid-connected hierarchical control strategy is established combined with tree-shaped and ring-shaped agent technology. Not only can it improve the utilization rate of household photovoltaics, but also it can reduce the adverse effects of photovoltaic and EV large-scale grid-connected in the traditional way. On the basis of participating in the load regulation of the distribution network, Prosumer can improve the stability of its power consumption.

INDEX TERMS Prosumer, energy management, smart load, multi-agent systems, distribution network.

I. INTRODUCTION

With the development of renewable energy and the continuous reduction of traditional energy, the global energy structure has changed dramatically. Household photovoltaic is widely favored for its advantages of low land cost, low transmission loss, and small investment in power transmission and transformation [1]–[3]. At the same time, electric vehicles become the trend of the future automobile industry because of the characteristics of cleanliness and environmental protection. The research on the charging technology of EV has also become a hot spot at home and abroad [4]–[6].

Traditional power systems were strictly divided into generation, transmission, distribution and consumption. However, with the development of distributed energy technology, consumers have the ability to produce and store electricity now. With the promotion of household photovoltaic and EV, the household electricity unit has become a hybrid of production and consumption of electricity, which is called Prosumer [7].

Therefore, it is necessary to manage and control Prosumer energy to reduce the adverse effects of grid voltage and frequency fluctuations on the operation of the Prosumer. Joakim M analyzed the probability distribution models of household electricity consumption, EV household charging power and household photovoltaic power generation respectively [8]. In view of the connection of PV Prosumers to microgrid, Nian Liu proposed Stackelberg game approach to carry out effective energy sharing management [9]. Based on this research, the method of using the energy of adjacent Prosumers containing PV was proposed to realize the sharing of energy storage equipment [10]. Masoud H.N proposed a Prosumer-based distributed frequency adjustment framework for power systems, but it only allowed each Prosumer to communicate with its neighbors [11]. Abbas Mehrabi proposed a charging/discharging scheduling mechanism for the EV connected to the household Prosumer, which was also used for the EV in multiple household public parking lots [12]. Based on multi-agent technology, Ye Cai proposed an energy distribution system, which encouraged each Prosumer to participate in regional load balancing [13]. Ranjan Pal transformed the real-time matching problem of Prosumer demand and grid supply into a stochastic optimization problem and proposed a fast-distributed MATCH real-time algorithm [14]. Rabiya Khalid proposed a hybrid Prosumer to Prosumer(P2P) energy trading model based on block chain, which eliminates the monopoly of the main grid by decentralizing the electricity trading market, and proposed a new bidding mechanism.

The associate editor coordinating the review of this manuscript and approving it for publication was Bin Zhou.

The proposed smart contract controls P2P and Prosumer to Grid (P2G) energy transactions during peak hours, reducing demand on the main grid while reducing peak average latency ratio (PAR) and power costs [15]. By modeling the energy transaction interaction between producers and consumers in virtual microgrid (VMG) as a producer-led Stackelberg game followed by consumers, Kelvin Anoh optimized the benefits of Prosumer [16]. Junjie Hu established virtual storage (VS) model for various distributed energy resources, and prosumers are further integrated by aggregators (Aggs) agent. Then, the Aggs' VS model and two-way power flow constraints is combined by the DSO, to determine the optimal day-ahead schedule of prosumers [17]. J P Iria proposed a two-stage stochastic optimization model to define the energy and tertiary reserve bid, which minimizes the net cost of purchasing and selling energy in the DA and RT markets and maximizes the revenue from selling tertiary reserves at the RT stage [18]. Armin Ghasem Azar used an alternate quote package production agreement and a reactive utility value concession strategy to enable virtual power plants and aggregators to negotiate a package of power and price quotes without knowing each other's preferences and utility functions [19].

Although more and more scholars have studied the Prosumer, there are still two aspects to be further explored in the research of household Prosumer energy management: (1) At present, most of the researches on Prosumer unit only consider P2G, and there are few P2P researches on the local energy flow market. The problem of power flow between multiple Prosumer units has not been well solved; (2) most existing researches use energy storage units to participate in energy management, and the high cost of energy storage units leads to a small number of users of Prosumer, which plays a limited role in reducing load fluctuations, reducing distribution network PAR and improving the operation stability of distribution network; (3) In traditional energy optimization methods, electrical appliances are mostly turned off or load shifted to improve the PAR to reduce energy consumption costs. On the one hand, the operation of the electrical equipment is inconvenient, on the other hand, it forces the users to change their habits of using electricity, which to some extent affects the users' experience of using electricity.

SL is composed of an electric spring (ES) in series with non-critical loads in the Prosumer (such as a household water heater, lighting system) of which the operating voltage can withstand a certain degree of deviation [20]. Nowadays, the flexible control method of SL's active power has been deeply studied [21]–[24], so it is certainly significant to use SL in the energy flow management of Prosumer.

In view of the above background, a method of Prosumer energy management based on smart load (SL) is proposed herein. The contribution of this paper is that: (1) an improved Prosumer power control model is firstly established based on the SL active power control method; (2) based on the PSO algorithm, the Prosumer real-time energy management method is proposed; (3) using multi-agent hierarchical control technology, a coordinated control strategy for multi-Prosumer grid connection is proposed. Finally, it is verified by simulation that the method described herein is effective. In the Prosumer model based on smart load proposed by us, the power consumption habits of users are not affected to the greatest extent and the power consumption cost of users is reduced.

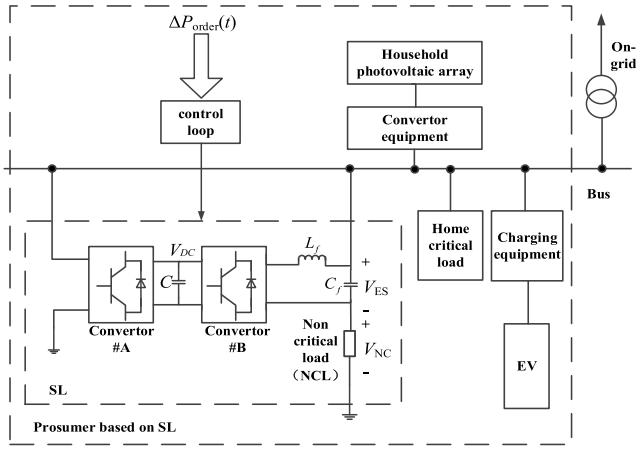

FIGURE 1. Prosumer structure model.

II. IMPROVED PROSUMER MODEL

Zafar Rehman explained the concept of Prosumer that it is a kind of users who are not just the power consumers, but also the power producers [25]. Household photovoltaic and EV are comprehensively considered to be added in the household Prosumer herein. Compared with the existing prosumer model, the proposed model increases the smart load (SL model) which is different from the traditional load. Based on the power models of the above units, ES is series connected with home non-critical load to form the SL model, as shown in Figure 1, then:

$$P_P = P_{PV} + P_{EV} + P_H + P_{SL} \tag{1}$$

In the formula (1), P_{P} is the overall power of the Prosumer; P_{PV} is the household photovoltaic power; P_{EV} is the charging power of household EV; P_{H} is the household critical load power; P_{SL} is the power of SL in the Prosumer. SL can support active and reactive power flow through decoupling control [23]. ES is composed of two back-to-back convertors and LC filters. Convertor #B is connected in series with NCL and acts as a series compensator to regulate the voltage and current injected by ES. It is connected to Convertor #A in parallel. The AC end of Convertor #A is connected to the power grid. As a shunt compensator, it regulates and keeps the V_{DC} of DC end unchanged. The common DC link is the power AC between Convertor #B and Convertor #A The channel is provided to realize the power balance in ES. The consumed power is marked in positive and the generated is negative herein. If the P_{P} value is positive, it indicates that the power consumed in the Prosumer is greater than the power generated

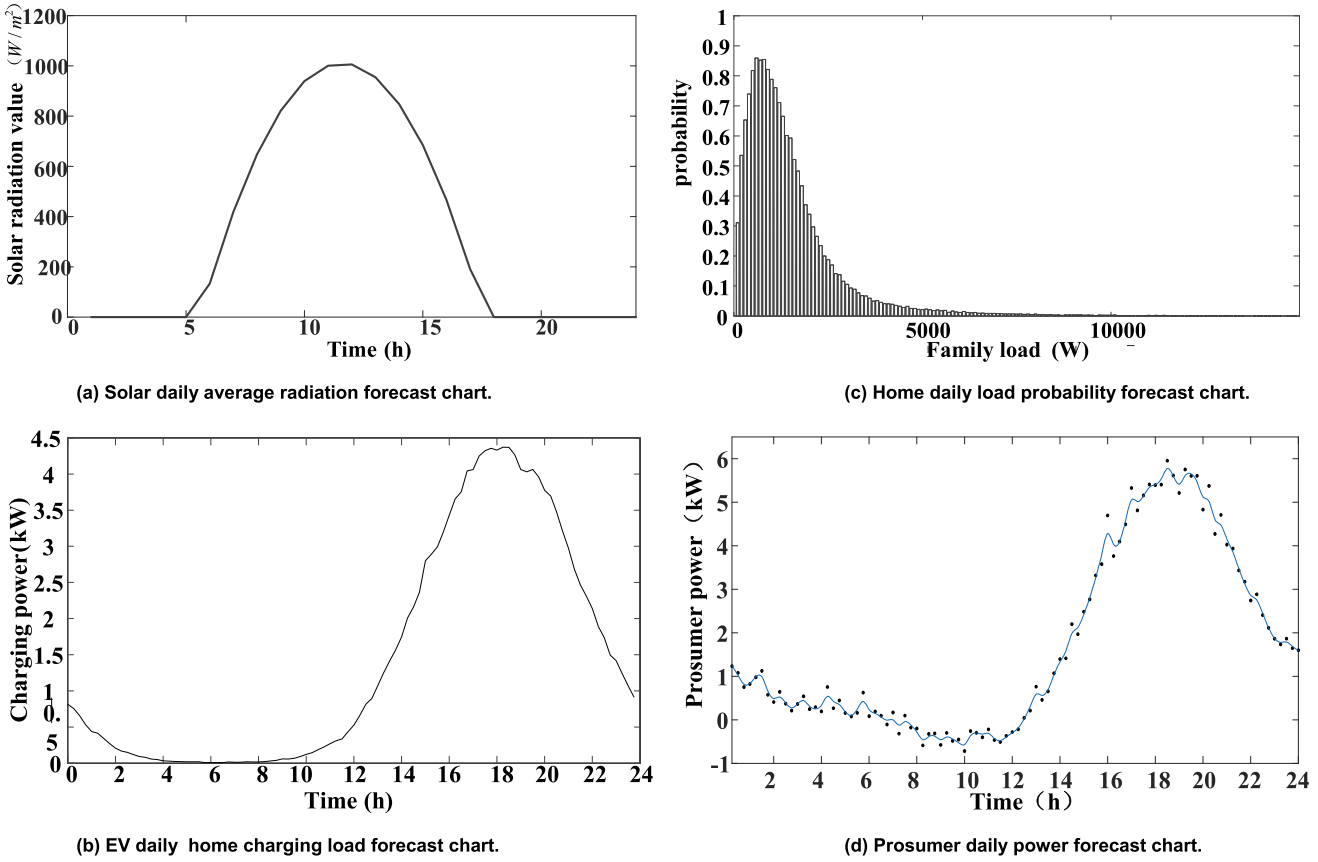

(a) Solar daily average radiation forecast chart.

(c) Home daily load probability forecast chart.

(b) EV daily home charging load forecast chart.

(d) Prosumer daily power forecast chart.

FIGURE 2. Daily power forecast of each part in Prosumer.

by the household photovoltaic. At this time, it needs to be supplied by the distribution network. Otherwise, it indicates that the generated power is greater than the consumed, which means the Prosumer can supply power to the distribution network.

The three-point solar radiation practical model is used to establish the power generation model of household photovoltaic in the Prosumer [26]. The three-point solar radiation practical model is based on the measured data of solar radiation to analyze the solar radiation characteristics of the whole day, and to simulate the solar radiation characteristics of the whole day based on the rising, setting and peak solar irradiance. According to this, the photovoltaic power generation capacity of the whole day is obtained. EV home charging load is forecast by modeling the initial charging time and the daily driving range [27]. The Monte Carlo simulation method is used to forecast the charging load P_{EV} of EV in one day. The Weibull probability distribution function is used to predict the home critical load power [28]. Therefore, the above predicted daily power results are shown in Figure 2(a), (b), (c), and when both EV and household photovoltaic are connected to the Prosumer, the daily load curve of Prosumer is as shown in Figure2(d).

Without the energy management control of the Prosumer, on one hand, the charging time of EV will overlap with the peak time of the household daily load to form a much higher load peak. On the other hand, it cannot maximize the use of photovoltaic power generation in Prosumer at noon time which will result in a larger peak-to-valley difference of household user and make adversely affects the stability of power grid.

III. PROSUMER DAILY REAL-TIME ENERGY MANAGE-MENT METHOD

SL can realize the continuous change of active power within a certain range. In order to solve the problem of bus voltage fluctuation caused by daily prediction power deviation of Prosumer unit, SL is used to adjust the overall active power of Prosumer to replace part of energy storage [28]. SL quadrant control method is used to control the active power of Prosumer, whose control phasor diagram is shown in Figure 3 [21].

Where, V_S is the supply voltage; V_{NCL}' and I_{ES}' are respectively the voltages and currents of non-critical loads before ES starts to work; V_{NCL} and I_{ES} are respectively the voltages and currents of non-critical loads after ES starts to work; V_{ES} is the voltage of ES. φ is the impedance angle of non-critical loads; θ is the phase of the converter modulated signal in SL (i.e, the phase angle of V leading I_{SL}).

According to Figure 3, in the case that active power of SL is controlled at the same time, the two working modes are as follows:

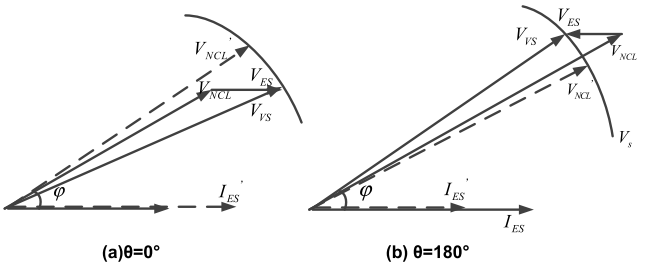

FIGURE 3. active power control phasor diagram based on SL.

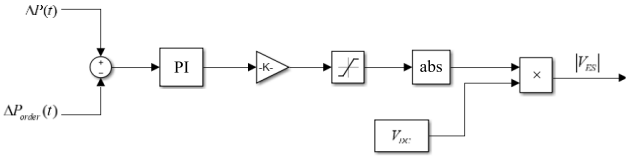

FIGURE 4. V_{ES} amplitude control loop.

A. Figure (a) shows the descent of active power mode to reduce the active power of SL.

B. Figure (b) shows the ascent of active power mode to increase the active power of SL.

The active power of an SL when it is not controlled can be expressed as equation (2):

$$P'_{SL} = \left|V'_{NCL}\right| \times \left|I'_{ES}\right| \times \cos\varphi \tag{2}$$

The active power of an SL when it is controlled can be expressed as equation (3):

$$P_{SL} = |V_{NCL}| \times |I_{ES}| \times \cos\varphi \tag{3}$$

According to Figure 1 and Figure 3 that the SL active power control models are respectively as equation (4):

$$\Delta P = P_{SL} - P'_{SL} = \frac{\cos\varphi}{|Z_{NCL}|} \times (|V_{VS} - V_{ES}|^2 - V_S^2) \tag{4}$$

Active power adjustment amount $\Delta P_{\text{order}}(t)$ in the t-th hour is obtained according to the demand of active power adjustment, and then the $\Delta P_{\text{order}}(t)$ instruction is sent to SL in the Prosumer. In equation (6), if the real-time instruction $\Delta P_{\text{order}}(t)$ is sent to SL, then:

$$|V_{SL} - V_{ES}|^2 = V_S^2 + \Delta P_{order}(t) \times \frac{|Z_{NCL}|}{\cos\varphi} \tag{5}$$

The amplitude of the V_{ES} can be changed dynamically to realize the control instruction $\Delta P_{\text{order}}(t)$. The angle of θ (0° or 180°) is switched according to the positive or negative of $\Delta P_{\text{order}}(t)$. The specific amplitude control loop of V_{ES} in Figure 1 is shown in Figure 4.

Among them, the demand of active power is determined by the minimization of the daily load fluctuation of the Prosumer, namely:

$$\min f = (\sum_{t=1}^{N} (P_P(t) - \overline{P_P})^2)/N \tag{6}$$

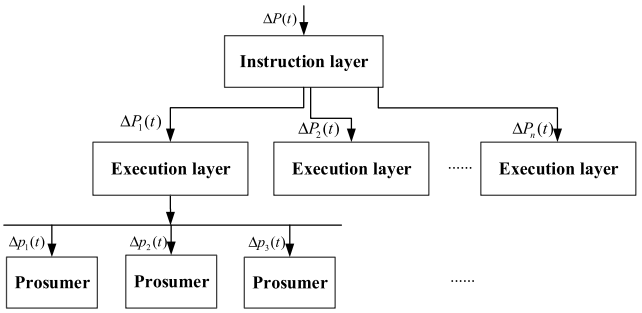

FIGURE 5. Hierarchical coordination control architecture of multi-Prosumers.

The constraint is:

$$\Delta P_{ES\_\min} \le \Delta P_{\text{order}}(t) \le \Delta P_{ES\_\max} \tag{7}$$

where $\Delta P_{\text{ES\_min}}$ and $\Delta P_{\text{ES\_max}}$ are the lower and higher limit of the active power adjustment capability of SL respectively. The lower limit of active power adjustment is $\Delta P_{\text{ES\_min}} = -\text{P}_{\text{NCLmax}}$, which represents the sum of rated active power of all non-critical loads. The upper limit of active power adjustment is $\Delta P_{\text{ES\_max}} = \text{P}_{\text{NCLmax}}$, which represents the maximum active power that all non-critical loads can bear.

Active power continuous control can be realized when the Prosumer executes the control instruction $\Delta P_{\text{order}}(t)$ through the SL, which can realize the flexible control of the entire active power of Prosumer.

IV. COORDINATED CONTROL STRATEGY OF MULTI-PROSUMERS

Considering that it is difficult for a large number of Prosumers to access the optimal control of distribution network at the same time, the tree-shaped agent and ring-shaped agent technology is used to hierarchical coordinated control Prosumers. The coordinated grid-connected control method of multi-Prosumers is mainly divided into two layers, that is instruction layer and execution layer. The instruction layer adopts tree-shaped agent control method, and the execution layer adopts ring-shaped agent control method. The Prosumers with similar distance in the area are connected by ring-shaped agent structure hand-in-hand. Then each ring-shaped Prosumer group is connected to the distribution network in tree-shaped agent structure to realize hierarchical and efficient control of the Prosumers. It can avoid the regional fault of the distribution network caused by the failure of an agent to complete the cooperation instructions of the superior. In the region, the ring-shaped agent composed of three Prosumers hand-in-hand is taken as an example, and its specific control architecture is shown in Figure 5.

$\Delta P(t)$ is the power control command issued by the distribution network to multi-Prosumer groups. $\Delta P_{\text{i}}(t)$ $(i = 1, 2, 3, \ldots)$ is the actual power value that the tree-shaped agent transmits to each ring-shaped Prosumer group after calculation by the upper agent control module. $\Delta p_{\text{j}}(t)(j = 1, 2, 3)$ is the required production/ consumption power value

of each Prosumer calculated by the lower level agent control module. This method can make full use of the renewable energy in the Prosumer to participate in the distribution network load regulation.

A. INSTRUCTION LAYER CONTROL STRATEGY

In fact, the instruction layer control problem of hierarchical coordinated control is to find the best value of $\Delta P_i(t)$, which is solved by PSO algorithm herein. According to the power control instruction $\Delta P(t)$ issued by the distribution network, the power value $\Delta P_i(t)$ required to be issued/absorbed by each ring-shaped agent group is solved, so that the sum of the adjustment of all ring-shaped agent groups has a small error with the adjustment instruction to be executed, so the objective function is:

$$\min f_1 = \left| \Delta P(t) - \sum_{i=1}^{n} \Delta P_i(t) \right| \tag{8}$$

where, $\Delta P_i(t)(i = 1, 2, 3, \ldots)$ is the real-time power of the i-th ring-shaped agent group; $P(t)$ is the real-time average power of all ring agent groups in the distribution network; n is the number of ring-shaped agent groups. When each ring-shaped agent group is connected to the grid, the power should be within its allowable range, that is, the constraint conditions:

$$\begin{cases} \Delta P_{1\_\min} \le \Delta P_1(t) \le \Delta P_{1\_\max} \\ \Delta P_{2\_\min} \le \Delta P_2(t) \le \Delta P_{2\_\max} \\ \qquad \cdots \\ \Delta P_{n\_\min} \le \Delta P_n(t) \le \Delta P_{n\_\max} \end{cases} \tag{9}$$

B. EXECUTION LAYER CONTROL STRATEGY

The problem of controlling execution layer is solving the power flow between the inter connected Prosumers in the region. After the local consumption of renewable energy is realized, the grid is connected with high efficiency and low cost. The power value that each Prosumer should produce/consume is obtained according to the command $\Delta P_i(t)$ given by the instruction layer. Since the power regulation quantity of each Prosumer is limited, the regulation instruction constraints of the ring-shaped agent are as follows:

$$\begin{cases} \Delta p_{1\_\min} \le \Delta \delta_1(t) \le \Delta p_{1\_\max} \\ \Delta p_{2\_\min} \le \Delta \delta_2(t) \le \Delta p_{2\_\max} \\ \qquad \cdots \\ \Delta p_{pnum\_\min} \le \Delta \delta_{pnum}(t) \le \Delta p_{pnum\_\max} \end{cases} \tag{10}$$

where, p_{num} represents the number of Prosumers in the agent of the ring-shaped Prosumer group; $\Delta p_{j\_\max}$ and $\Delta p_{j\_\min}$ represent the upper and lower limits of the acceptable active power regulation instructions of the j-th Prosumer respectively; $\Delta \delta_j(j = 1, 2, \ldots, p_{num})$ is the total number of real-time control instructions of the j-th Prosumer, that is:

$$\Delta \delta_j(t) = \Delta p_j(t) + \Delta p_{j(j-1)}(t) + \Delta p_{j(j+1)}(t) \tag{11}$$

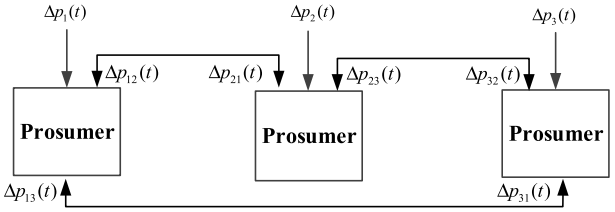

FIGURE 6. Cooperative control architecture of lower level agent.

Combined with the control instructions given by the instruction layer center and the power adjustment limits of each Prosumer, the final power value that each Prosumer should produce/consume is obtained. The control structure of the ring-shaped agent with such a hand-in-hand can solve the control strategy response problem after a Prosumer stops responding for some reason. The cooperative control architecture is shown in Figure 6.

The specific steps are as follows.

(1) Accept the instruction layer control instruction $\Delta P_i(t)$, and give each Prosumer to accept the upper control instruction:

$$\Delta p_j(t) = \Delta P_i(t)/pnum \tag{12}$$

(2) Judge whether the j-th Prosumer in the ring-shaped Prosumer group can accept the control instruction, if it can, it will operate normally; if not, it will obtain the instruction that it needs to cooperate with the regulation:

$$\begin{cases} \Delta p_j(t) = a \\ \Delta p_{j(j-1)} = b \\ \Delta p_{j(j+1)} = c \end{cases} \tag{13}$$

Moreover, because the j-th unit refuses to accept the instruction, the link regulation power between the $(j-1)$-th unit and the $(j+1)$-th unit is directly assigned as 0, that is, it does not participate in the optimal regulation of the lower level load fluctuation minimization of the Prosumer group.

(3) Transmit the stop operation signal of the j-th Prosumer to the (j-1)-th and ($j+1$)-th Prosumers, and request each auxiliary to share partial power command quantities $\Delta p_{j(j+1)}(t)$ and $\Delta p_{j(j-1)}(t)$ of a/2.

(4) After superposing the auxiliary shared power instruction quantity of the (j-1)-th and (j+1)-th Prosumers, check whether it is out of limit. If it is out of limit, transfer the out of limit part instruction to the (j-2)-th Prosumer and the (j+2)-th Prosumer, and so on.

V. TEST VERIFICATION

In the above, an improved Prosumer model is established including electric vehicle charging technology and household photovoltaic technology, and a real-time energy management method of Prosumer is proposed based on SL power control model. Then, a hierarchical energy coordinated control method for grid connection of multi-Prosumers are studied by using tree-shaped and ring-shaped multi-agent technology.

TABLE 1. Specific parameters of SL.

Symbol	Value
NCL impedance (ZNCL)	20+j20Ω
NCL Rated active power (PNCL-N)	2400W
ΔP_{ES_min}	-2000W
ΔP_{ES_max}	2000W

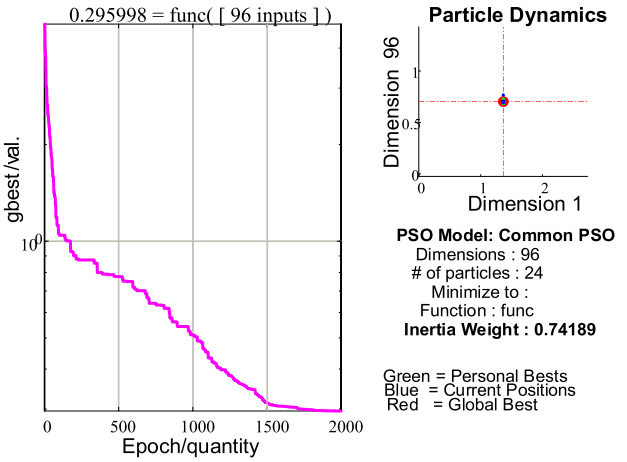

FIGURE 7. PSO process of Prosumer.

In this section, based on MATLB/Simulink, the simulation model and the hardware in the loop simulation are established to verify the above methods step by step.

First, establish the simulation model as shown in Figure 1 and assume that the specific parameters of SL in the Prosumer are as shown in Table 1. Using PSO algorithm, the control instruction $\Delta P_{\text{order}}(t)$ needed to be executed by the Prosumer is obtained according to the previous day's experience data. The specific PSO process is shown in Figure 7, which can minimize the daily load fluctuation of Prosumer.

However, due to the influence of prediction error, the $\Delta P_{\text{order}}(t)$ required in real time may be different from the day-ahead calculation value. The real-time data is used to carry out the quadratic optimization of the day-ahead calculated $\Delta P_{\text{order}}(t)$. The real-time $\Delta P_{\text{order}}(t)$ after quadratic optimization obtained according to Figure 7 is shown in Figure 8, and the control instruction to be executed is passed to the SL execution unit. The active power value $\Delta P_P(t)$ adjusted according to the instruction is shown in Figure 9. The adjusted power of Prosumer needed from grid is shown in Figure 10.

Compared with Figure 8 and Figure 9, the actual real-time active power adjustment value of Prosumer is more consistent with the required output/absorption power value and meets the upper and lower limit constraints of SL in each time period. Compared with the adjustment instructions that need to be executed, the adjustment curve of the active power of the actual Prosumer is relatively smooth, and the smooth control of the Prosumer can effectively prevent the failure of the

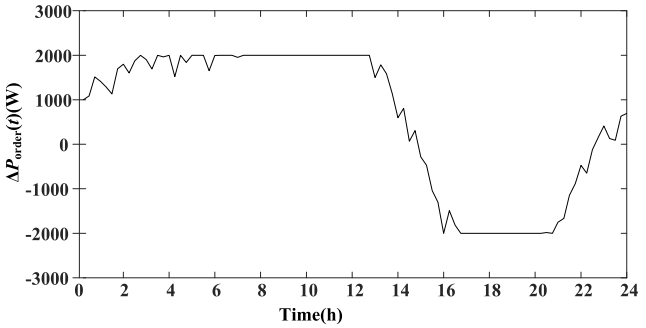

FIGURE 8. Adjustment instruction $\Delta P_{order}(t)$ to be executed by Prosumer.

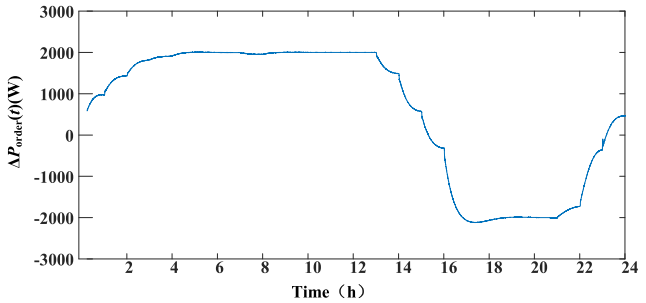

FIGURE 9. Real-time active power adjustment value $\Delta P_{order}(t)$ of Prosumer.

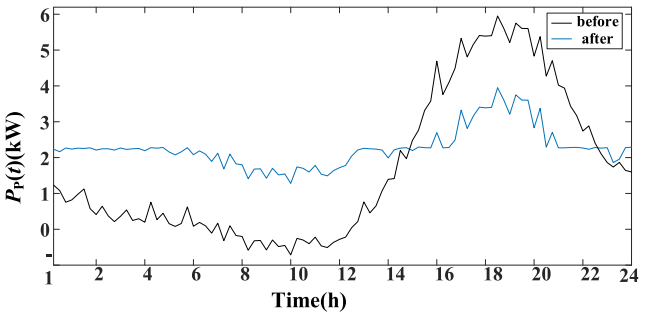

FIGURE 10. Real-time $P_P(t)$ of Prosumer before and after adjustment.

non-critical load equipment of the Prosumer due to the sudden increase and decrease of the control instructions.

A. SIMULATION OF MULTI-PROSUMERS GRID-CONNECTED HIERARCHICAL COORDINATED CONTROL

Grid-connected hierarchical coordinated control of multi-Prosumers is mainly divided into upper tree-shaped agent control strategy and lower ring-shaped agent control strategy. As shown in Figure11, the simulation model is IEEE13 node system with low-voltage extended network. There is a 4.16/480V transformer between the 633 and 634 nodes of the system, which is responsible for converting the higher transmission voltage to the lower distribution voltage. After the 634 node, a 480/220V transformer is responsible for converting the 480V distribution voltage to the 220V terminal area voltage. The power flow model between each ring-shaped

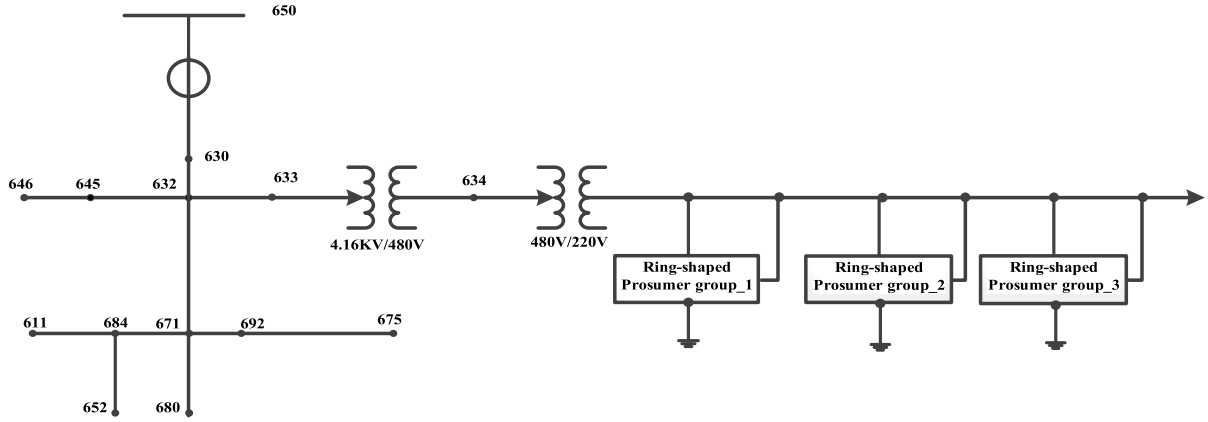

FIGURE 11. Grid-connection simulation model of multi-Prosumers.

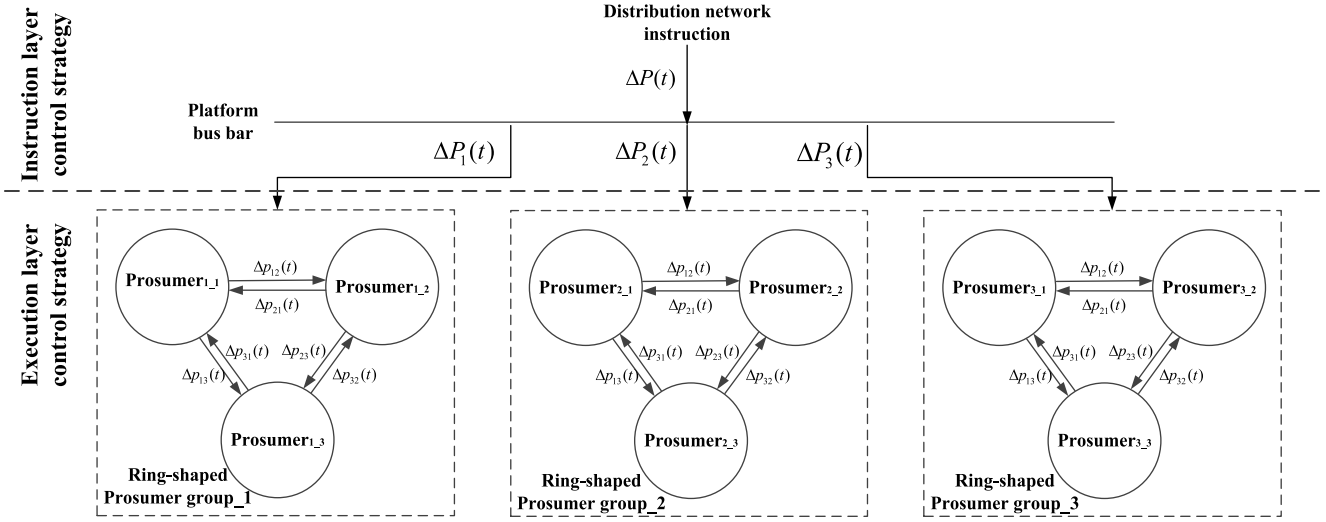

FIGURE 12. Hierarchical coordinated control model for grid-connection of multi-Prosumers.

prosumer group in Figure 11 and between each ring-shaped Prosumer group and the control center of the upper platform area is shown in Figure12.

It is assumed that there are three ring-shaped Prosumer groups in the station area, and each ring-shaped Prosumer group is composed of three Prosumers. The specific parameters are shown in TABLE 2.

1) VERIFICATION OF INSTRUCTION LAYER CONTROL STRATEGY

The upper tree agent control mainly uses PSO algorithm to distribute the power control instruction $\Delta P(t)$ issued by the distribution network reasonably according to the regulation restrictions of different ring agent groups, so that the sum of the adjustment of all ring agent groups has a small error with the regulation instructions to be executed. According to Table 1, it can be assumed that the upper and lower limits of the power of the ring-shaped Prosumer group_1, ring-shaped Prosumer group_2 and ring-shaped Prosumer group_3 are

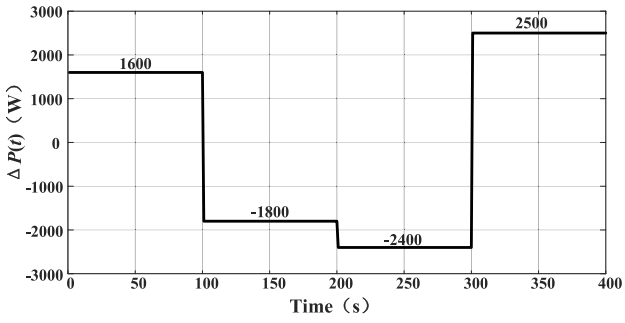

FIGURE 13. Total power adjustment instruction $\Delta P(t)$.

[−650, 950]W, [−1150, 1150]W and [−950, 750]W respectively. It is assumed that the power adjustment instruction $\Delta P(t)$ of the substation area issued by the distribution network is as shown in Figure 13.

According to the regulation instruction setting in Figure 13, conduct the simulation for 400s, and use PSO algo-

TABLE 2. Specific parameters of Prosumer group.

Ring-shaped Prosumer group_1	$Prosumer_{1\_1}$ Upper and lower limits of power $[\Delta P_{11\_min}, \Delta P_{11\_max}]$	[-200,400]W
	$Prosumer_{1\_2}$ Upper and lower limits of power $[\Delta P_{12\_min}, \Delta P_{12\_max}]$	[-200,200]W
	$Prosumer_{1\_3}$ Upper and lower limits of power $[\Delta P_{13\_min}, \Delta P_{13\_max}]$	[-250,350]W
Ring-shaped Prosumer group _2	$Prosumer_{2\_1}$ Upper and lower limits of power $[\Delta P_{21\_min}, \Delta P_{21\_max}]$	[-300,300]W
	$Prosumer_{2\_2}$ Upper and lower limits of power $[\Delta P_{22\_min}, \Delta P_{22\_max}]$	[-450,450]W
	$Prosumer_{2\_3}$ Upper and lower limits of power $[\Delta P_{23\_min}, \Delta P_{23\_max}]$	[-400,400]W
Ring-shaped Prosumer group _3	$Prosumer_{3\_1}$ Upper and lower limits of power $[\Delta P_{31\_min}, \Delta P_{31\_max}]$	[-300,250]W
	$Prosumer_{3\_2}$ Upper and lower limits of power $[\Delta P_{32\_min}, \Delta P_{32\_max}]$	[-300,200]W
	$Prosumer_{3\_3}$ Upper and lower limits of power $[\Delta P_{33\_min}, \Delta P_{33\_max}]$	[-350,300]W

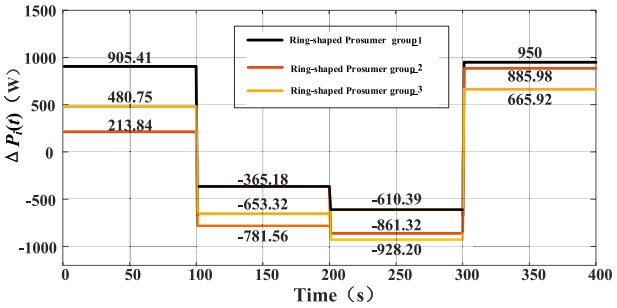

FIGURE 14. Active power value $\Delta P_i(t)$ required to be produced/consumed by each ring-shaped prosumer group.

rithm to get the power value $\Delta P_i(t)$ required to be sent out/absorbed by each ring-shaped prosumer group, as shown in Figure 14.

2) VERIFICATION OF EXECUTION LAYER CONTROL STRATEGY

According to the active power $\Delta P_i(t)$ required to be produced /consumed by each ring-shaped Prosumer group, the control strategy of execution layer proposed above is verified taking the ring-shaped Prosumer group_1 as an example. For example, in 0-100s, the ring-shaped Prosumer group_1 needs to generate 905.41W active power, which is evenly distributed to the three included Prosumers, then each unit needs to generate 301.80W active power. However, according to Table 1, if the upper and lower limits of the acceptable regulation instructions of the $Prosumer_{1\_1}$ are $[-200, 200]$W, it is unable to complete all the regulation instructions, and it is necessary to seek help from the $Prosumer_{1\_1}$ and the $Prosumer_{1\_3}$ to share the active power by 50.9W. The active power value $\Delta p_i(t)$ needed to be produced /consumed by each Prosumer in real time in 400s is obtained by analogy as shown in Figure 15.

Through MATLAB/Simulink simulation, the control command of the execution layer is given to the SL control unit in

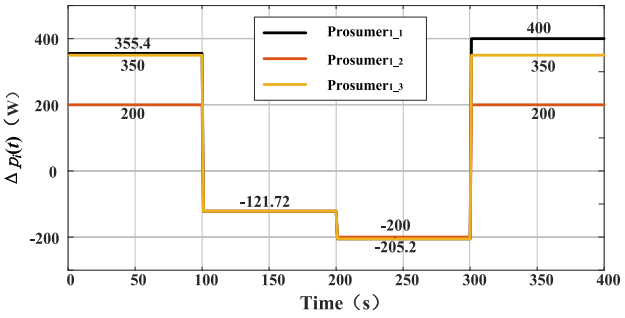

FIGURE 15. Active power value $\Delta p_i(t)$ required to be produced/consumed by each Prosumer.

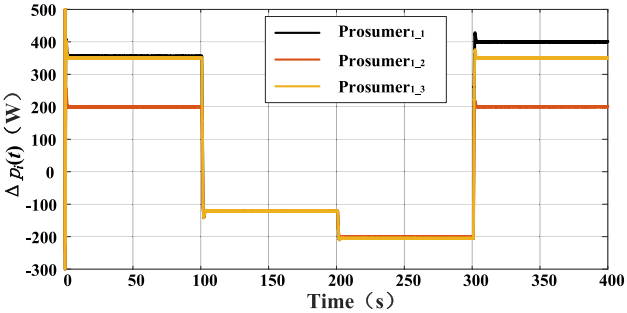

FIGURE 16. Actual power value of three units' SL $\Delta P_i(t)$.

each Prosumer, and the simulation time is 400s. The actual power values of the three units SL are shown in Figure 16, which are very consistent with the power values required to be produced /consumed in Figure 14, and $\Delta p_i(t)$ meets the upper and lower limits of power constraints shown in Table 2 in each time period.

The actual power values of the three units are superposed to get the total power values of the actual three units participating in the regulation, as shown in Figure 17. The instruction $\Delta P_1(t)$ shown in Figure 12 distributed by the PSO algorithm of the lower level control is basically consistent with that transmitted from the upper level control, which shows that the multi-level coordinated control strategy for grid connection of the Prosumers is effective.

B. HARDWARE SIMULATION OF MULTI-PROSUMERS COORDINATED CONTROL METHOD

In view of the coordination control method of multiple Prosumer units mentioned above, semi-physical simulation was carried out again for verification, and the voltage was set to 220V. The physical simulation diagram is shown in Figure 18. The SL labels of three prosumer units are set as (1), (2) and (3), respectively, and their NCL rated active power is 1209.93w, 967.66w and 1000w, respectively. The SL power constraints in the three units are shown in the annular prosumer $group_{1\_1}$ power constraints in table 2. Three converter # A is shown as tag (4), (5) and (6), and three converter # B is shown as tag (7), (8) and (9). And choose DSP

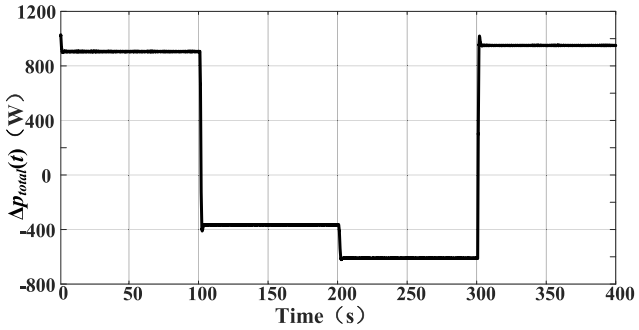

FIGURE 17. Actual total active power value $\Delta p_{total}(t)$ of circular Prosumer group_1.

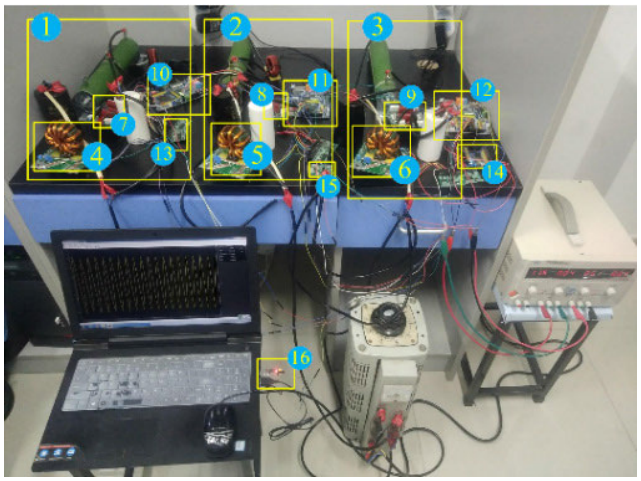

FIGURE 18. Experimental device.

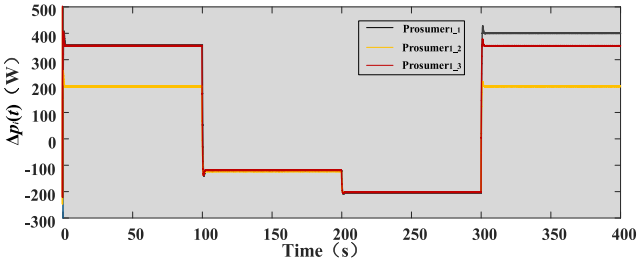

FIGURE 19. Actual SL power value $\Delta p_i(t)$ of experimental results.

F28335 as the executive level controller for tags (10), (11) and (12). IR2110 chip (tag (13)) and DSP F28335 integration are selected to drive the converter. MSP430 is selected as instruction layer controller (14) (tag). Tag (15) is the power measurement circuit, and power supply information transmitted to computer through the TTL - USB interface (tag (16)).

According to the control method of the execution layer, the active power needed to be sent out/absorbed by the lower unit group is shown in Figure 14. Set the test time to 400s, and get the actual active power of three Prosumers as shown in Figure 19.

Combined with Figure 16 and Figure 19, it can be found that the actual regulation power of each Prosumer in the ring-shaped Prosumer group is consistent with the theoretical simulation results. It is also verified that the improved Prosumer by using SL can effectively control the power flow of the Prosumer in real time. After the control center of the instruction layer and the execution layer, the distribution network instructions are effectively transmitted to each Prosumer in real time. At the same time, each Prosumer is involved in the power regulation of the distribution network in the substation area, so as to relieve the pressure of the peak load of the distribution network power.

VI. CONCLUSION

In conclusion, this paper proposes a SL based Prosumer energy management method, which fully considers the uncertainty of distributed energy such as household photovoltaic and electric vehicles. Firstly, based on the PSO algorithm, the energy scheduling is optimized according to the day-ahead predicted value. Then, based on the active power control method of SL, the real-time power control model of Prosumer was established, and the real-time energy management method of users was proposed to reduce the influence of prediction error. Based on the hierarchical control technology of tree and ring agents, the coordinated control strategy of multi-user network connection is proposed. Finally, through MATLAB/Simulink simulation and hardware simulation, it is verified that the active power control method of SL can effectively realize the real-time control of user power and reduce the daily load fluctuation of users. In addition, according to the real-time energy management method of Prosumer, the effectiveness of the guidance layer control strategy and the executive layer control strategy are verified respectively. It also proves that the distribution network directive can reach each Prosumer in the region quickly, so that it can fully participate in the load regulation and control of the distribution network, and realize the improvement of renewable energy efficiency.

REFERENCES

[1] J. Pan, H. Wu, and D. Xu, "Capacity optimization of rooftop photovoltaic based on photovoltaic/electric vehicle/load game," *Autom. Electr. Power Syst.*, vol. 43, no. 1, pp. 186–197, Oct. 2018, doi: 10.7500/AEPS20180422006

[2] Y. Wang, X. Lin, and M. Pedram, "A near-optimal model-based control algorithm for households equipped with residential photovoltaic power generation and energy storage systems," *IEEE Trans. Sustain. Energy*, vol. 7, no. 1, pp. 77–86, Jan. 2016, doi: 10.1109/TSTE.2015.2467190.

[3] E. Yao, P. Samadi, V. W. S. Wong, and R. Schober, "Residential demand side management under high penetration of rooftop photovoltaic units," *IEEE Trans. Smart Grid*, vol. 7, no. 3, pp. 1597–1608, May 2016, doi: 10.1109/TSG.2015.2472523.

[4] Z. Pan, C. Gao, and S. Liu, "Research on charging and discharging dispatch of electric vehicles based on demand side discharge bidding," *Power Syst. Technol.*, vol. 40, no. 4, pp. 1140–1146, Apr. 2016, doi: 1000-3673(2016)04-1140-07.

[5] M. S. Islam, N. Mithulananthan, and D. Q. Hung, "A day-ahead forecasting model for probabilistic EV charging loads at business premises," *IEEE Trans. Sustain. Energy*, vol. 9, no. 2, pp. 741–753, Apr. 2018, doi: 10.1109/TSTE.2017.2759781.

[6] W. Yi, W. Feihong, and H. Xingzhe, "Random access control strategy of charging for household electric vehicle residential area," *Autom. Electr. Power Syst.*, vol. 42, no. 20, pp. 53–60, Oct. 2018, doi: 10.7500/AEPS20180409007.

[7] A. C. Luna, N. L. Diaz, M. Graells, J. C. Vasquez, and J. M. Guerrero, "Cooperative energy management for a cluster of households prosumers," *IEEE Trans. Consum. Electron.*, vol. 62, no. 3, pp. 235–242, Aug. 2016, doi: 10.1109/TCE.2016.7613189.

[8] J. Munkhammar, J. Widén, and J. Rydén, "On a probability distribution model combining household power consumption, electric vehicle home-charging and photovoltaic power production," *Appl. Energy*, vol. 142, pp. 135–143, Mar. 2015, 10.1016/j.apenergy.2014.12.031.

[9] N. Liu, X. Yu, C. Wang, and J. Wang, "Energy sharing management for microgrids with PV prosumers: A stackelberg game approach," *IEEE Trans. Ind. Informat.*, vol. 13, no. 3, pp. 1088–1098, Jun. 2017, doi: 10.1109/TII.2017.2654302.

[10] N. Liu, M. Cheng, X. Yu, J. Zhong, and J. Lei, "Energy-sharing provider for PV prosumer clusters: A hybrid approach using stochastic programming and Stackelberg game," *IEEE Trans. Ind. Electron.*, vol. 65, no. 8, pp. 6740–6750, Aug. 2018, doi: 10.1109/TIE.2018.2793181.

[11] M. H. Nazari, Z. Costello, M. J. Feizollahi, S. Grijalva, and M. Egerstedt, "Distributed frequency control of prosumer-based electric energy systems," *IEEE Trans. Power Syst.*, vol. 29, no. 6, pp. 2934–2942, Mar. 2014, doi: 10.1109/TPWRS.2014.2310176.

[12] A. Mehrabi and K. Kim, "Low-complexity charging/discharging scheduling for electric vehicles at home and common lots for smart households prosumers," *IEEE Trans. Consum. Electron.*, vol. 64, no. 3, pp. 348–355, Aug. 2018, doi: 10.1109/TCE.2018.2864548.

[13] Y. Cai, T. Huang, E. Bompard, Y. Cao, and Y. Li, "Self-sustainable community of electricity prosumers in the emerging distribution system," *IEEE Trans. Smart Grid*, vol. 8, no. 5, pp. 2207–2216, Sep. 2017, doi: 10.1109/TSG.2016.2518241.

[14] R. Pal, C. Chelmis, M. Frincu, and V. Prasanna, "MATCH for the prosumer smart grid the algorithmics of real-time power balance," *IEEE Trans. Parallel Distrib. Syst.*, vol. 27, no. 12, pp. 3532–3546, Dec. 2016.

[15] R. Khalid, N. Javaid, A. Almogren, M. U. Javed, S. Javaid, and M. Zuair, "A blockchain-based load balancing in decentralized hybrid P2P energy trading market in smart grid," *IEEE Access*, vol. 8, pp. 47047–47062, Mar. 2020, doi: 10.1109/ACCESS.2020.2979051.

[16] K. Anoh, S. Maharjan, A. Ikpehai, Y. Zhang, and B. Adebisi, "Energy peer-to-peer trading in virtual microgrids in smart grids: A game-theoretic approach," *IEEE Trans. Smart Grid*, vol. 11, no. 2, pp. 1264–1275, Mar. 2020, doi: 10.1109/TSG.2019.2934830.

[17] J. Hu, Y. Li, and H. Zhou, "Energy management strategy for a society of prosumers under the IOT environment considering the network constraints," *IEEE Access*, vol. 7, pp. 57760–57768, Apr. 2019, doi: 10.1109/ACCESS.2019.2913724.

[18] J. P. Iria, F. J. Soares, and M. A. Matos, "Trading small prosumers flexibility in the energy and tertiary reserve markets," *IEEE Trans. Smart Grid*, vol. 10, no. 3, pp. 2371–2382, May 2019, doi: 10.1109/TSG.2018.2797001.

[19] A. G. Azar, H. Nazaripouya, B. Khaki, C.-C. Chu, R. Gadh, and R. H. Jacobsen, "A non-cooperative framework for coordinating a neighborhood of distributed prosumers," *IEEE Trans. Ind. Informat.*, vol. 15, no. 5, pp. 2523–2534, May 2019, doi: 10.1109/TII.2018.2867748.

[20] G. Ma, G. Xu, Y. Chen, and R. Ju, "Voltage stability control method of electric springs based on adaptive PI controller," *Int. J. Electr. Power Energy Syst.*, vol. 95, pp. 202–212, Feb. 2018, doi: 10.1016/j.ijepes.2017.08.029.

[21] Y. Chen, G. Ma, Y. Wang, and G. Xu, "An adaptive voltage-regulation control strategy of an electric spring based on output current feedback," *IEEJ Trans. Electr. Electron. Eng.*, vol. 14, no. 3, pp. 394–402, Mar. 2019, doi: 10.1002/tee.22820.

[22] K.-T. Mok, S.-C. Tan, and S. Y. R. Hui, "Decoupled power angle and voltage control of electric springs," *IEEE Trans. Power Electron.*, vol. 31, no. 2, pp. 1216–1229, Feb. 2016, doi: 10.1109/TPEL.2015.2424153.

[23] Q. Wang, M. Cheng, Y. Jiang, W. Zuo, and G. Buja, "A simple active and reactive power control for applications of single-phase electric springs," *IEEE Trans. Ind. Electron.*, vol. 65, no. 8, pp. 6291–6300, Aug. 2018, doi: 10.1109/TIE.2018.2793201.

[24] J. Soni and S. K. Panda, "Electric spring for voltage and power stability and power factor correction," *IEEE Trans. Ind. Appl.*, vol. 53, no. 4, pp. 3871–3879, Aug. 2017, doi: 10.1109/TIA.2017.2681971.

[25] R. Zafar, A. Mahmood, S. Razzaq, W. Ali, U. Naeem, and K. Shehzad, "Prosumer based energy management and sharing in smart grid," *Renew. Sustain. Energy Rev.*, vol. 82, pp. 1675–1684, Feb. 2018, doi: 10.1016/j.rser.2017.07.018.

[26] X. Qingshan, Z. Haixiang, and B. Haihong, "Establishment and feasibility researches of practical solar radiation model," (in Chinese), *Acta Energiae Solaris Sinica*, vol. 32, no. 8, pp. 1180–1185, 2011.

[27] K. Chaudhari, N. K. Kandasamy, A. Krishnan, A. Ukil, and H. B. Gooi, "Agent-based aggregated behavior modeling for electric vehicle charging load," *IEEE Trans. Ind. Informat.*, vol. 15, no. 2, pp. 856–868, Feb. 2019, doi: 10.1109/TII.2018.2823321.

[28] J. Munkhammar, J. Rydén, and J. Widén, "Characterizing probability density distributions for household electricity load profiles from high-resolution electricity use data," *Appl. Energy*, vol. 135, pp. 382–390, Dec. 2014, doi: 10.1016/j.apenergy.2014.08.093.

GANG MA was born in Shandong, China. He received the B.S., M.S., and Ph.D. degrees from North China Electric Power University, Beijing, China, in 2008, 2013, and 2013, respectively. Since 2013, he has engaged in teaching and scientific research of power systems and relay protection. He is currently an Associate Professor with Nanjing Normal University. His current research interests include power system analysis, renewable energy resources, and fault diagnosis related technologies.

JIE LYU was born in Henan, China. She received the B.Eng. degree in electrical engineering from North China Electric Power University, Beijing, China, in 2016. She is currently pursuing the M.S. degree in electrical engineering with Nanjing Normal University, Nanjing, China. Her research interests include renewable power generation, power system analysis, and demand side response.

YING WANG was born in Jiangsu, China. She received the B.Eng. degree in electrical engineering from Southeast University, Nanjing, China, in 2017. She is currently pursuing the M.S. degree in electrical engineering with Nanjing Normal University, Nanjing. Her research interests include renewable power generation and power system analysis.

JIAN ZHANG was born in Jiangsu, China. He received the B.S. degree from the Huaiyin Institute of Technology, Huai'an, China, in 2018. He is currently pursuing the M.S. degree with Nanjing Normal University, Nanjing. His current research interests include power systems, demand response, and power electronics.

JIE XU was born in Jiangsu, China. She received the B.S. degree from the Beijing Institute of Petrochemical Technology, Beijing, China, in 1998, and the M.S. and Ph.D. degrees from the Nanjing University of Aeronautics and Astronautics, Nanjing, China, in 2011. She is currently an Associate Professor with Nanjing Normal University. Her current research interests include fault detection and diagnosis, reliable control, and industrial process monitoring.